Saudi Journal of Biological Sciences 29 (2022) 2270–2279

Contents lists available at ScienceDirect

Saudi Journal of Biological Sciences

journal homepage: www.sciencedirect.com

Original article

Green synthesis of zinc oxide nanoparticles using *Anoectochilus elatus*, and their biomedical applications

Natesan Vijayakumar [a], Venkataesan Kumari Bhuvaneshwari [a], Gandhimathi Kaliyamoorthi Ayyadurai [b], Rajendran Jayaprakash [c], Kasi Gopinath [d,*], Marcello Nicoletti [e], Saud Alarifi [f], Marimuthu Govindarajan [g,h]

[a] *Department of Biochemistry and Biotechnology, Faculty of Science, Annamalai University, Annamalainagar 608002, Tamilnadu, India*
[b] *Department of Chemistry, Sri Sairam Engineering College, Sai Leo Nagar, West Tambaram, Chennai 600044, Tamilnadu, India*
[c] *Department of Chemistry, School of Arts and Science, Aarupadai Veedu Institute of Technology, Vinayaka Mission's Research Foundation (Deemed to be University), Paiyanoor 603104, Tamilnadu, India*
[d] *Department of Packaging, Yonsei University, 1 Yonseidae-gil, Wonju-si, Gangwon-do 26493, South Korea*
[e] *Department of Environmental Biology, Sapienza University of Rome, Rome 00185, Italy*
[f] *Department of Zoology, College of Science, King Saud University, Riyadh 11451, Saudi Arabia*
[g] *Unit of Mycology and Parasitology, Department of Zoology, Annamalai University, Annamalainagar-608 002, Tamilnadu, India*
[h] *Unit of Natural Products and Nanotechnology, Department of Zoology, Government College for Women (Autonomous), Kumbakonam 612 001, Tamilnadu, India*

ARTICLE INFO

Article history:
Received 29 September 2021
Revised 14 November 2021
Accepted 28 November 2021
Available online 3 December 2021

Keywords:
Anoectochilus elatus
Nanotechnology
Zinc Oxide nanoparticles
Antimicrobial activity
Anti-inflammatory activity

ABSTRACT

Zinc and its derivatives requirement increased to enhance human immunity against the different pandemics, including covid-19. Green synthesis is an emerging field of research. Zinc oxide (ZnO) nanoparticles have been prepared from *Anoectochilus elatus* and characterized using absorption, vibrational and electron microscope analysis. They were carried for antibacterial, inflammatory control tendency, and potential antioxidant activities. The brine shrimp lethal assay tested the biologically derived nanomaterial toxicity and the lethal concentration (LC_{50}) is 599.79 μg/ml. The inhibition against the important disease-causing pathogens was measured against four-gram negative, gram-positive bacteria and two fungus pathogens. The nanomaterial exposed inhibition zone for gram-positive bacteria between 17 mm and 25 mm. The inhibition zone against gram-negative bacteria exists between 19 mm and 24 mm. The anti-inflammatory activity was assessed by inhibition of protein denaturation and protease inhibitory activity using nanomaterial. The antioxidant activity was examined using four assays for the therapeutic activities. The average size range of 60–80 nm nanoparticles has prepared and exposed the good biological activity between 50 μg/ml and 100 μg/ml. The comparative results of anti-inflammatory and antioxidant assay results with standards such as Aspirin and vitamin C exposed that two to three times higher concentrations are required for the fifty percent of inhibitions. The prepared low-cost nanoparticle has exhibited excellent biological activity without any side effects and may enhance immunity.

1. Introduction

Green synthesis has received more attention for various applications because of the low-cost, eco-friendly, safe nanoparticles (NPs) preparation (Govindarajan et al., 2016a,b; Govindarajan and Benelli, 2017; Balalakshmi et al., 2017; Suganya et al., 2017; Balasooriya et al., 2017). Due to the size and shape of the nanomaterials, they have shown various applications in medicinal fields (Narayanan and Sakthivel, 2011). Synthesis of new molecules using the biosynthetic technique is a growing field and the method using bio-extracts has expected more responsiveness than chemical and physical methods for the nanomaterial preparation (Iravani, 2011).

* Corresponding author.
E-mail address: gloriousnanogopi@gmail.com (K. Gopinath).

Peer review under responsibility of King Saud University.

Production and hosting by Elsevier

https://doi.org/10.1016/j.sjbs.2021.11.065
1319-562X/

Therefore, there is a growing need for substituent or alternate approaches with various requirements such as eco-safe and cost-effective. Green synthesis is an effective nanoparticle synthesis method, which is inexpensive with risk-free, hypo-allergic within a step synthesis (Rosi and Mirkin, 2005). Nanotechnology is a field of research about less than 100 nm size particles with the distribution, morphology (Senthilkumar et al., 2017). The new method required overcoming the exorbitant, utilizing toxic chemicals imposing environmental and biological risks of the various nanoparticle synthesis methods such as precipitation, electrodeposition, chemical, hydrothermal, sol-gel, and microwave-assisted combustion no chemical techniques (Li et al., 2014).

Based on the reported research of silver NPs by green synthesis and green nanotechnology review, nano synthesis was carried for the green method's biological applications (Jagtap and Bapat, 2013; Roy et al., 2013; Nath and Banerjee, 2013). It was reported that several biological organisms such as bacteria, plants and fungus were used for the synthesis of metal oxide NPs by simple methods and had more advantages over conventional physico-chemical methods (Gunalan et al., 2012; Ahmad et al., 2019; Raja et al., 2018). Zinc is an essential trace metal. Recent reports indicate that the NPs, including Zinc oxide nanoparticles (ZnONPs) synthesized by the green technique, was non-toxic, bio-safe, biocompatible, and had good inhibition against various microorganisms compared to chemically derived nanoparticles (Agi et al., 2020; Cheng et al., 2020; Naseer et al., 2020). The ZnONPs by the green technique can be used for drug delivery purposes (Kalpana and Devi Rajeswari, 2018; Selim et al., 2020). The phytoremediation was explained for plants' green synthesis of NPs (Husen and Siddiqi, 2014; Baharara et al., 2014; Priyanka and Prasanna, 2020). Since ancient times medicinal plants were widely used in the traditional phytotherapy with various herbal formulations despite all the controversy concerning their efficacy and safety, which believed to be an important source of various phytoconstituents such as saponins, alkaloids, terpenes, flavonoids and glycosides due to their potential therapeutic effects (Fugh, 2000; Mathivanan et al., 2010; Govindarajan, 2011; Govindarajan et al., 2013; Govindarajan and Benelli, 2016).

Due to various bioactive metabolites such as flavonoids, alkaloids, saponins, glycosides, terpenoids and steroids present in the plants, which act as significant pharmaceutical potential action as antidiabetic, anticancer, anti-inflammatory, anti-malarial and anti-dysentery properties and in this present covid-19 pandemic situation, the plants and their extracts act as one of the major sources of drugs in both modern and traditional system of medicine (Yuan et al., 2016; Arumugam et al., 2016). It was reported that the use of non-toxic materials like plant extracts and bacteria for the synthesis of zinc nanoparticles offers various benefits in the field of pharmaceuticals.

Nowadays, metal-based NPs are evolving as new drug carriers that provide a way for site-specific targeting and drug delivery (Ajithadas et al., 2015). *Anoectochilus elatus* Lindl. (Nagathali) is belongs to the family Orchidaceae. Orchids require nutrients include more than 30,000 species of 750 genera approximately (Jin-Ming et al., 2003) and new ones are being revealed in tropical areas. Several orchids are used in traditional medicine for several ailments, also called Jewel orchids, supporting their anticancer activity.

World Health Organisation also supports the practice of traditional medicine for its safety and efficacy. *A. elatus* species have been used in the traditional medical system to treat hypertension, respiratory, liver, chest diseases and abdominal pains. So, there is a demand for the species with medicinal and ornamental value. In this background, our study was designed to synthesize and characterize ZnONPs using *A. elatus* and evaluate theirs *in vitro* brine shrimp lethal assay, antimicrobial, anti-inflammatory, and antioxidant activities.

2. Materials and methods

2.1. Materials

All the chemicals and the microbiological media were obtained from Himedia, India. Ultrapure MilliQ water was used throughout the study. All bacterial and fungus strains were purchased from the American-type culture collection.

2.2. Collection and extraction of A. elatus leaf

A. elatus was collected from the region around Kolli hills, Tamilnadu, India and Botanist authenticated it. Then the air-dried plant leaves ground well. The dried plant powder was extracted in water and concentrated after the charcoal treatment. Fifty grams of whole leaf powder yielded 8.0 g after being dried under a vacuum and stored in a refrigerator.

2.3. Qualitative phytochemical analysis of A. elatus leaf extract

The *A. elatus* leaf extracts were subjected to qualitative analysis for phenolic groups, glycosides, alkaloids, flavonoids, tannins, terpenoids, saponins steroids by using different solvents,

2.4. Synthesis of Zinc oxide nanoparticles

50 ml of aqueous extract of *A. elatus* was heated to 60 °C and then 5 g in 50 ml water solution of zinc nitrate was added slowly to the extract at the same temperature. The reaction mixture was heated until it transformed into a deep yellow suspension. After 4 h, the paste was transferred in a ceramic crucible and the formed ZnONPs of *A. elatus* (*Ae*-ZnONPs) was washed by hot water. Then, the sample was heated in an air heated furnace at 100 °C for 2 h. A light white coloured powder was obtained after heating the powder in a muffle furnace at 400 °C for 3 h and carried for the characterization (Doan et al., 2020).

2.5. Characterization of Ae-ZnONPs

The adsorption spectrum of *Ae*-ZnONPs was analyzed in between 200 and 450 nm range in the UV–Visible spectrophotometer. The vibrational behaviour of the nanoparticles was investigated using the Thermo Nicolet FTIR model iS5 Spectrophotometer. The prepared test specimen surface was captured by using Philips XL30 Scanning Electron Microscope.

2.6. Brine shrimp lethal assay

The *in vivo* brine shrimp lethal assay in seawater was investigated for the prepared *Ae*-ZnONPs and lethal concentration for fifty percent mortality (LC_{50}) was calculated (Jayaprakash et al., 2016).

2.7. Antimicrobial activity of Ae-ZnONPs

The antimicrobial effects of the *Ae*-ZnONPs against totally eight bacterial strains and two fungal strains were used throughout the investigation. The bacteria used were *Bacillus subtilis, Staphylococcus aureus, E. coli, Pseudomonas aerogenosa, Enterococcus faecalis, Micrococcus luteus, Shigella fluxneri*, and *Serratia marcescens*. The fungal strains used were *Aspergillus niger* and *Candida albicans*. The bacterial culture inoculation of microorganisms was prepared for the assay as per the reported method (Janaki et al., 2015).

The *Ae*-ZnONPs (10 mg/ml) solution was prepared in sterile distilled water. Different concentrations, maximum of 100 μl extract, were transferred into wells using sterile Pasteur pipettes. Incuba-

tion completed at 37 °C for 24 h plates outcomes were examined for the effectiveness. Antimicrobial activities were estimated by determining the growth-controlled zone area in diameters. The susceptibility test was carried using standard Ciprofloxacin (100 μg/ml) for the bacterial pathogens and Amphotericin B (100 μg/ml) (Alastruey et al., 2015) for the fungus study as a positive control. The inhibition zone was measured in millimeters and compared.

2.8. Anti-inflammatory activity of Ae-ZnONPs

In vitro anti-inflammatory studies analyzed the suppression of both inflammation and arthritis of *Ae*-ZnONPs by inhibition of albumin denaturation was performed by the reported methods (Pant et al., 2012) and membrane stabilization test using Alsever mixture (Anosike et al., 2012).

2.9. Antioxidant activity of Ae-ZnONPs

The effect of *in vitro* antioxidant potential activities of *Ae*-ZnONPs was studied using free radical scavenging activity such as 1-diphenyl-2-picrylhydrazyl (DPPH) (Chowdhury et al., 2014), reducing potential, 2, 2′-azino-bis (3-ethylbenzthiazoline-6-sulfo nic acid) (ABTS) (Kumari et al., 2016), hydrogen peroxide methods (Gülçin et al., 2010). A Nitric oxide (NO) scavenging assay was performed using sodium nitroprusside, which can be determined using the Griess-Illosvoy reaction.

3. Results

3.1. Phytochemical studies

The prepared *A. elatus* leaves extracts using ethanol, benzene, petroleum ether, chloroform, and water were screened for the presence of different phytoconstituents shown in Fig. 1 and Table 1**.** The result exposed that the polar solvents consist of all phytoconstituents except oil, gums & mucilage, chlorogenic compound and remaining exhibit the minimum chemicals.

3.2. Characterization of Ae-ZnONPs

Optical characterization of the *Ae*-ZnONPs was carried out using a UV–Visible absorption spectrophotometer in the range of 200–700 nm. The recorded UV spectrum of *Ae*-ZnONPs has two peaks at 275 nm, 380 nm, respectively (Fig. 2a). Tauc plot values obtained from the UV data also coincide with the reported values for *Ae*-ZnONPs. 275 nm and 386 nm exposed the bandgap energy of 2.54 eV, 3.12 eV, respectively. Tauc plot was drawn by the online tool (https://www. instanano. com/ 2020/ 05/draw-tauc-plot-from-UV–vis-absorbance.html) using UV data and the plotted Tauc plot between Energy and $(\alpha h\nu)^2$ using UV data in origin which has shown in Fig. 2b. Vibrational spectroscopy has been used to study the ZnO bonding in nanoparticles. FTIR of *Ae*-ZnONPs is presented in Fig. 2c. From the recorded vibrational spectra, major peaks are observed at 3429 cm^{-1}, 1389 cm^{-1}, 1119 cm^{-1}, 619 $cm^{-1}$and 480 cm^{-1}. Strong broadband at 480 cm-1 is denoted for a pure ZnO bond.

The absorption band for O—H stretching vibration of water molecule was detected at 3429 cm^{-1}. The Zn-O stretching for the absorption band is exhibited between 450 cm^{-1} and 500 cm^{-1} for ZnO nanoparticles and is almost coincidental with the reported value. The bond nature was confirmed by force constantly. It was calculated by the online tool (https://www.instanano.com/2020/03/force-constant-calculator-from-ftir.html) and the values are presented in Table.2. The scanning electron microscope (SEM) image of synthesized *Ae*-ZnONPs is displayed in Fig. 2d. The SEM image reveals the powder form of the *Ae*-ZnONPs and the layers are observed in the morphology. On the surface, macroporous nature was noticed.

3.3. LC_{50} calculation

The preliminary toxicity limit of the *Ae*-ZnONPs was studied by BSLA method. For the serially diluted samples, the percentage of mortality was calculated and shown in Table.3. The concentration versus % of mortality graph plotted with regression calculation and lethal concentration for 50% (LC50) was measured. The regression graph is shown in Fig. 3. The *Ae*-ZnONPs exposed the higher LC_{50} of 599.79 μg/ml, valuable data for further drug-oriented studies within the limit.

3.4. Antimicrobial activities of Ae-ZnONPs

The antibacterial activity of the *Ae*-ZnONPs showed a significant reduction in bacterial growth in terms of zone of inhibition. The anti-fungal activity of *Ae*-ZnONPs against the plant and human disease-causing pathogens such as *Candida albicans, Aspergillus nigar* using serially diluted solutions and compared with usual standard. The inhibition zone observed for both the pathogens is 18 mm, 13 mm, respectively. The results of serially diluted inhibition zones are presented in Table.4. The test plates and comparison chart of the inhibition zones are shown in Fig. 4a and b**.**

Fig. 1. Phytochemical analysis of *Anoectochilus elatus.*

Table 1
Phytochemical constituents of different extracts of *Anoectochilus elatus* leaves.

S. No.	Test for	Aqueous	Ethanol	Benzene	Petroleum ether	Chloroform
1.	Alkaloid	++	+	ND	ND	ND
2.	Flavonoid	++ +	++	+	++	+
3.	Triterpenoid	++	++	+	ND	+
4.	Phenolic compound	+++	+	+++	+	+
5.	Protein	+	+	+	+	+
6.	Carbohydrates	+	+	ND	ND	ND
7.	Saponin	+++	++	+++	–	++
8.	Steroids	+++	++	+	+	ND
9.	Glycosides	++	+	ND	ND	+
10.	Amino acid	+	+	+	ND	+
11.	Tannin	+++	++	++	+	+
12.	Oil	ND	ND	ND	ND	ND
13.	Gums &mucilage	ND	ND	ND	ND	ND
14.	Chlorogenic compound	ND	ND	ND	ND	ND

+++ = high; ++ = moderate; + = low; ND = not detectable.

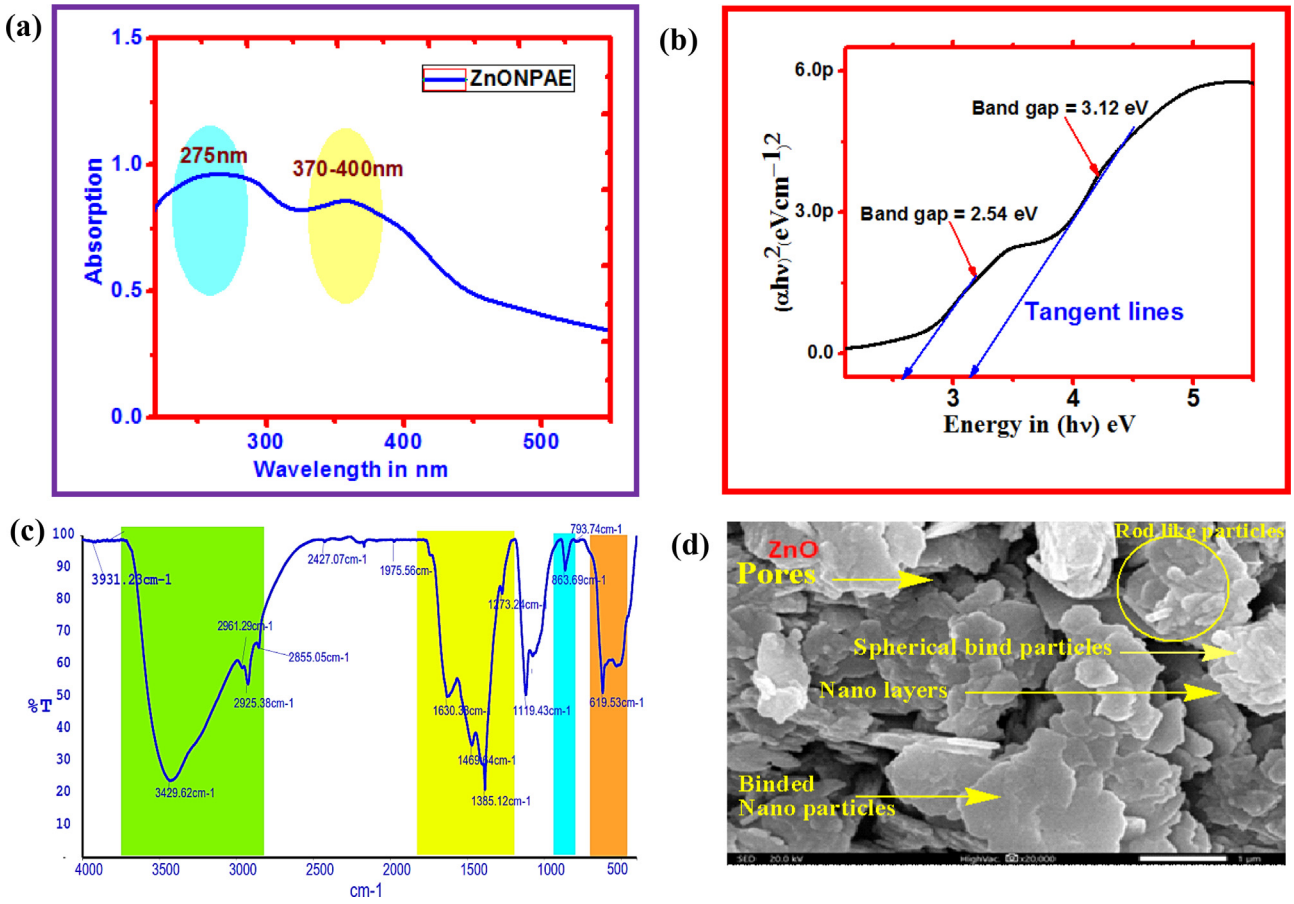

Fig. 2. Characterization of *Ae*-ZnONPs. (a) UV spectra; (b) Tauc plot; (c) FTIR spectra; (d) SEM image.

Table 2
Online calculated Force constant for the IR frequency.

Frequency	Force Constant in dyne/cm	
	Single bond	Double bond
3429	8,957,414	517,914,829
1385	1461326.5	2922652.9
1119	953911.0	1907822.1
863	567373.8	1134747.6
619	291896.6	583793.1

Table 3
BSLA result.

Conc. in μg/ml	Number of Mortality	% of Mortality	LC_{50} (μg/ml)
62.5	0	0 ± 0.000	599.79
125	0	0 ± 0.000	
250	3	15 ± 0.013	
500	11	40 ± 0.000	
1000	16	90 ± 0.942	

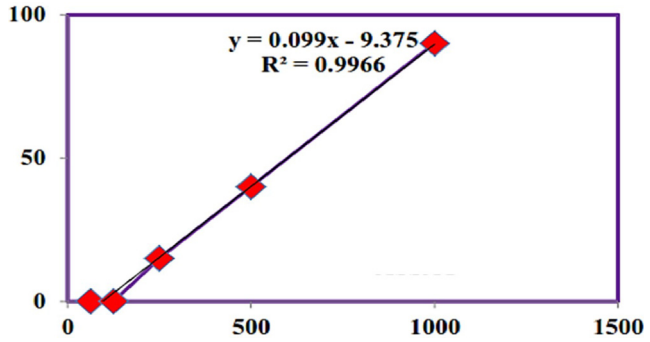

Fig. 3. Regression graph of BSLA.

3.5. In vitro anti-inflammatory effect of Ae-ZnONPs

3.5.1. Inhibition of albumin denaturation

Denaturation of proteins is well-documented due to the cause of inflammation. As part of the investigation on the mechanism of the anti-inflammation activity, the ability of serially diluted *Ae*-ZnONPs protein denaturation was studied. It was active in impeding the albumin denaturation by induced heat effect. The results for the serially diluted test samples are presented in Table 5. The Maximum inhibition of 76.02% was observed for *Ae*-ZnONPs and the standard aspirin drug showed the maximum inhibition of 86% inhibition for 50 μg/ml concentrations. The result obtained from the regression graph (Fig. 5) and the calculated IC_{50} value of Albumin denaturation is 63 μg/ml.

3.5.2. Membrane stabilization test

Similarly, like albumin denaturation, test samples (10–100 μg/ml) inhibited the heat-induced haemolysis of RBCs to a varying degree, as shown in Table. 5. It showed the maximum inhibition of 80.06 ± 0.37% at 100 μg/ml. Using the regression graph equation (Fig. 5), IC_{50} was observed at 53 μg/ml. Standard aspirin drug showed the maximum inhibition, 88.92% at 50 μg/ml.

3.6. Radical scavenging activity of Ae-ZnONPs

3.6.1. DPPH assay

The DPPH radical scavenging activity was detected and compared with ascorbic acid. The activity of DPPH radical scavenging of *Ae*-ZnONPs and ascorbic acid was shown in Table. 6 and Fig. 6a. The inhibition % for serial concentration like 20, 40, 60, 80 and 100 μg/ml was observed such as 38.11 ± 0.2, 52.39 ± 1.3, 69.03 ± 0.2, 80.15 ± 0.9 and 92.74 ± 0.3. However, for ascorbic acid were found to be 42.27 ± 1.5, 59.08 ± 0.5, 71.56 ± 1.0, 83.40 ± 0.7, and 95.01 ± 0.3 for serial dilution of maximum 50 μg/ml. From the plotted regression graph, IC_{50} values for DPPH scavenging activity for *Ae*-ZnONPs and Vit-C were 35 μg/ml, 14 μg/ml, respectively.

3.6.2. Reducing power assay

Potential antioxidant activity can be measured from its reducing tendency of a compound. The Fe^{3+} to Fe^{2+} transformation was investigated in the presence of the *Ae*-ZnONPs to reduce power activity. Similar to the other antioxidant assays, the reducing power of *Ae*-ZnONPs increased with increasing dosage. Table 7 shows the percentage of inhibition results of the nanoparticles and the standard. A regression graph (Fig. 6b) was plotted and IC_{50} was calculated for both.

3.6.3. Hydrogen peroxide radical assay

Table 8 and Fig. 6c shows the control percentage of H_2O_2 with serial concentrations such as 20, 40, 60, 80 and 100 μg/ml were observed in 66.94 ± 1.6, 51.04 ± 0.5, 38.26 ± 0.3, 23.02 ± 0.7, and 17.46 ± 0.2 respectively. Likewise, the inhibition percentage of Vitamin-C for 10, 20, 30, 40 and 50 μg/ml were found to be 24.10 ± 0.3, 40.42 ± 1.2, 52.0.9 ± 0.7, 64.36 ± 1.5 and 78.62 ± 0.4.

3.6.4. Nitric oxide assay

The percentage of inhibition in the nitric oxide of different concentrations was measured and compared with the same standard Vitamin-C. The outcomes after the colorimetric estimation were tabulated and presented in Table 9. They were using the inhibition percentage regression equation calculated from the graph (Fig. 6d). The IC_{50} values for nitric oxide scavenging activity for *Ae*-ZnONPs and Vit-C were 62 μg/ml and 16 μg/ml, respectively. The ratio between the two IC_{50} values was 3.9 times which showed higher concentration when compared to other ratios.

4. Discussion

The qualitative data of *A. elatus* reveals the presence of various secondary metabolites such as alkaloids, flavonoids, phenols, tannins, saponins and steroids. The spectrum showed a resemblance with the reported UV of ZnO nanoparticles (Talam et al., 2012). The observed narrowing peaks confirmed the reduction of zinc nitrate into ZnONPs. These two peaks exposed the nano nature of ZnO nanoparticles. The observed band gap energy values are almost coincidence with the cubic ZnO and wurtzite ZnONPs was 3.692 keV, 3.691 keV, respectively. In FTIR, the higher values

Table 4
Antimicrobial activity of *Ae*-ZnONPs.

S. No.	Microorganisms	Zone of inhibition (mm)				
		100 μg/ml	75 μg/ml	50 μg/ml	25 μg/ml	Standard*
Gram-Positive Bacteria						
1.	*Bacillus subtilis*	25	23	20	15	21
2.	*Staphylococcus aureus*	19	17	15	13	24
3.	*Enterococcus faecalis*	20	18	16	11	22
4.	*Micrococcus luteus*	17	16	14	12	25
Gram-Negative Bacteria						
5.	*E. coli*	24	20	17	14	26
6.	*Pseudomonas aeruginosa*	19	17	14	10	22
7.	*Serratiamercescens*	21	16	17	13	23
8.	*Shigellaflexneri*	22	19	16	12	24
	Fungal strains					
9.	*Candida albicans*	18	16	14	11	22
10.	*Aspergillusnigar*	13	11	10	08	20

* Ciprofloxacin (100 μg/ml) for the bacterial pathogens and Amphotericin B (100 μg/ml) for the fungus study as a positive control.

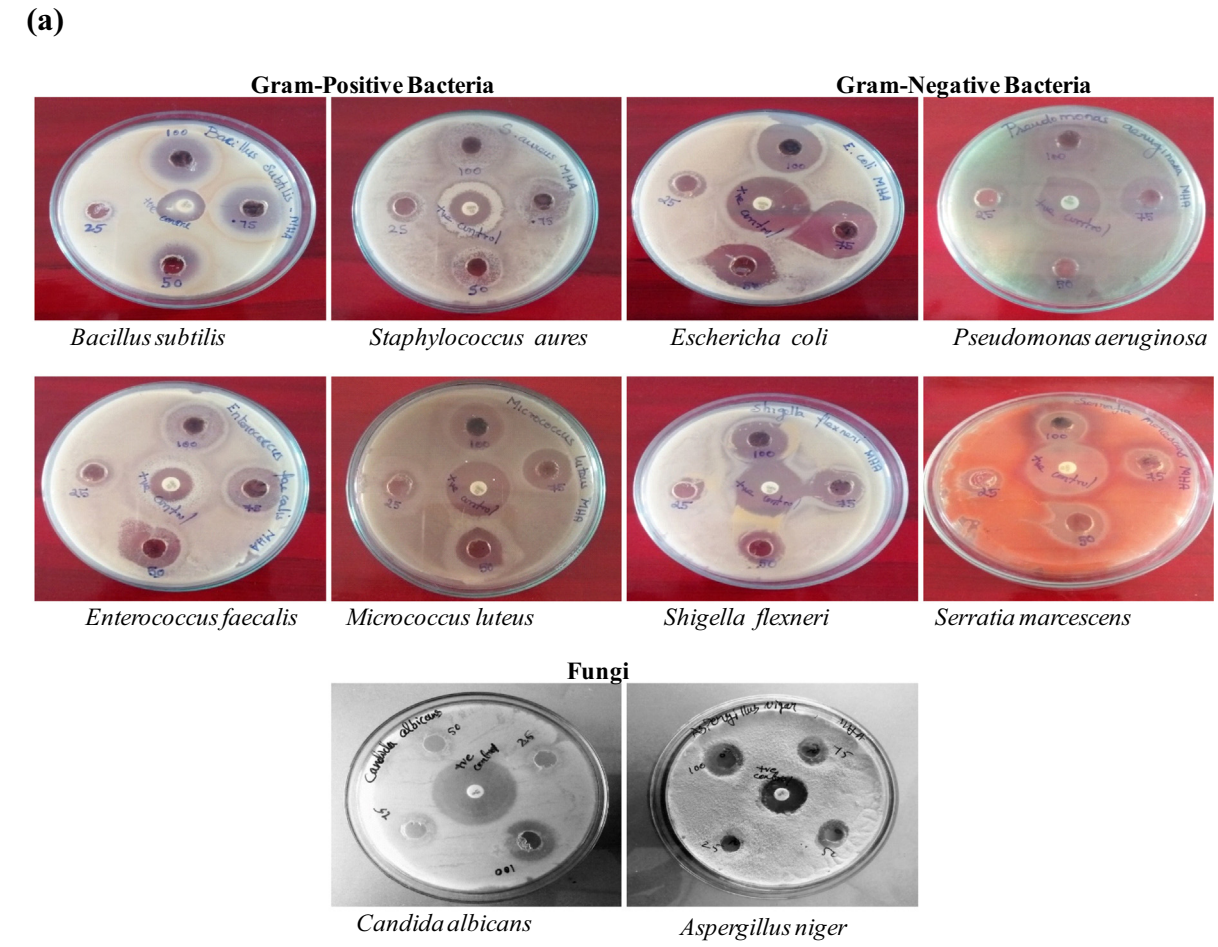

Fig 4. (a) Anti-microbial activity of *Ae*-ZnONPs; (b) Comparison chart of the inhibition zones.

showed the strong bond nature of ZnONPs. The force of the one atom on the other atom based on the molecular weight was higher in the ZnONPs. The higher elongation property of the nanoparticles may be the reason for the higher penetrating tendency of the nanoparticles into the cell. Due to the higher concentration, the morphology of the *Ae*-ZnONPs is changed to layers. The surface morphology is merely a coincidence with the reported morphology (Bodke et al., 2018). Somewhere, the particles have shown spherical and rod-like structures (Indramahalakshmi, 2017).

The *Ae*-ZnONPs showed dose-dependent activity with an increase in the concentration of nanoparticles. *Ae*-ZnONPs and their ability to bind with the cell membrane generate reactive oxy-

Table 5
Anti-inflammatory activity of *Ae*-ZnONPs.

S. No.	Treatment	Test Conc. (μg/ml)	% Inhibition	
			Albumin denaturation	Membrane stabilization
1.	*Ae*-ZnONPs	100	76.02 ± 0.31	80.06 ± 0.37
		80	62.46 ± 1.16	69.02 ± 1.6
		60	47.83 ± 0.09	55.91 ± 0.49
		40	34.31 ± 1.07	40.90 ± 0.21
		20	18.73 ± 1.46	26.27 ± 0.32
2.	Aspirin	50	86.00 ± 0.54	88.92 ± 0.37
		25	71.35 ± 1.06	76.22 ± 1.18
IC_{50}			63 μg/ml.	53 μg/ml

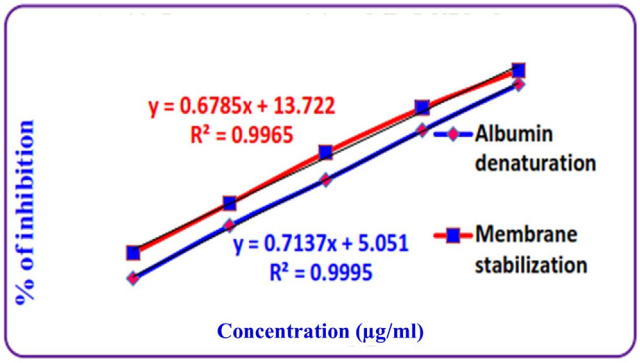

Fig. 5. Anti-inflammatory activity of *Ae*-ZnONPs.

Table 6
DPPH radical scavenging activity of *Ae*-ZnONPs.

Treatment	Concentration (μg/ml)	% of inhibition	IC_{50} value (μg/ml)
Ae-ZnONPs	100	92.74 ± 0.3	35
	80	80.15 ± 0.9	
	60	69.03 ± 0.2	
	40	52.39 ± 1.3	
	20	38.11 ± 0.2	
Vitamin- C	50	95.01 ± 0.3	14
	40	83.40 ± 0.7	
	30	71.56 ± 1.0	
	20	59.08 ± 0.5	
	10	42.27 ± 1.5	

gen species (ROS), thus enhancing the efficacy against drug-resistant bacterial strains (Bruska et al., 2011). The effects of *Ae*-ZnONPs were more potent against gram-positive bacterial strains as compared to gram-negative strains. The *Ae*-ZnONPs have revealed more potent bactericidal activity against gram-positive *Enterococcus faecalis* and *Micrococcus luteus* than gram-negative, *Shigella flexneri* and *E. coli,* respectively. *Ae*-ZnONPs can be selected as an antibacterial material because of their superior properties, such as high specific surface area and high activity to block a broad scope of pathogenic agents (Sirelkhatim et al., 2015). It also exposed the inhibition zone for gram-positive bacteria between 17 mm and 25 mm and showed 4 mm more inhibition zone against *Bacillus subtilis* when compared with standard.

Similarly, the *Ae*-ZnONPs exhibited a reasonable zone of inhibition against gram-negative bacteria. The inhibition zone exists between 19 mm and 24 mm. The zones are less than 2 to 3 mm when compared to standard ciprofloxacin. This result confirmed the reported research of the ZnONPs inhibition tendency against gram-positive bacteria (Wei et al., 2009; Mariappan et al., 2011). These zones are less than the standard and better for *Candida albicans.* Biologically synthesized *Ae*-ZnONPs nanomaterial showed better results against the selected pathogens, useful for future or impregnated drugs (Faraz et al., 2018).

Although the precise mechanism of this membrane stabilization is yet to be elucidated, it may be possible that the *Ae*-ZnONPs produced this effect through the surface area/volume ratio of the cells, which could be brought about by an expansion of membrane or the shrinkage of the cells and interaction with membrane proteins (Alenghat, 2013; Christopher et al., 2015). This work observed the coincidence in the results, which showed a slight difference in inhibition from the comparison**.** This exposed the triplicated trials are almost accurate in results.

The higher inhibition activity was recorded in *A. elatus* dose-dependent (Rahman et al., 2015). The outcomes exposed double the concentration required for the 50% inhibition of the free radical and confirmed the effective control of free radicals of stable DPPH. The *Ae*-ZnONPs exhibits the IC_{50} = 5673 μg/ml and the calculated ratio with the standard is 2.1 times (Irshad et al., 2012). The result shows that *Ae*-ZnONPs showed good reducing power when compared to the standard. The IC_{50} values for hydrogen peroxide scavenging activity for *Ae*-ZnONPs and Vitamin-C were 76 μg/ml, 28 μg/ml, respectively (Chen et al., 2007). The statistical value of triplicated trials exposed the ratio of IC_{50} is 2.71 between *Ae*-ZnONPs and Vitamin-C, which showed the resemblance with DPPH assay ratio 2.5. The *Ae*-ZnONPs meritoriously reduced the formation of nitric oxide from sodium nitroprusside. Inhibition increased with the increasing concentration of the extract (Sonane et al., 2017). A free radical's product in mammalian cells is Nitric oxide, which regulates various physical processes. However, excess nitric oxide production is interconnected with numerous diseases (Ponvinobala et al., 2012; Gangwar et al., 2014). The results almost showed the resemblances which denote the accuracy of the test trials.

5. Conclusion

The present study was formulated to understand the phytochemical analysis, biologically synthesis of nanoparticles, phytochemical analysis, characterization, BSLA toxicity, antimicrobial, anti-inflammatory, and potential antioxidant activities of *Ae*-ZnONPs. The green synthesized *Ae*-ZnONPs revealed for its characterization studies by UV, FTIR and SEM. The prepared nanoparticle characterization reports are almost similar to the earlier reported results. The nanoparticle behaviour was confirmed through characterization. The synthesized nanoparticles exhibited low toxicity against the brine shrimp. Also, it possesses significant antimicrobial activity and can be alternating existing antimicrobial agents. Due to particle permeability, the particles exposed good antimicrobial inhibition zones against all kinds of selected pathogens and better against the thicker walls containing gram-positive pathogens. The zones are less than 2 to 3 mm compared to standard

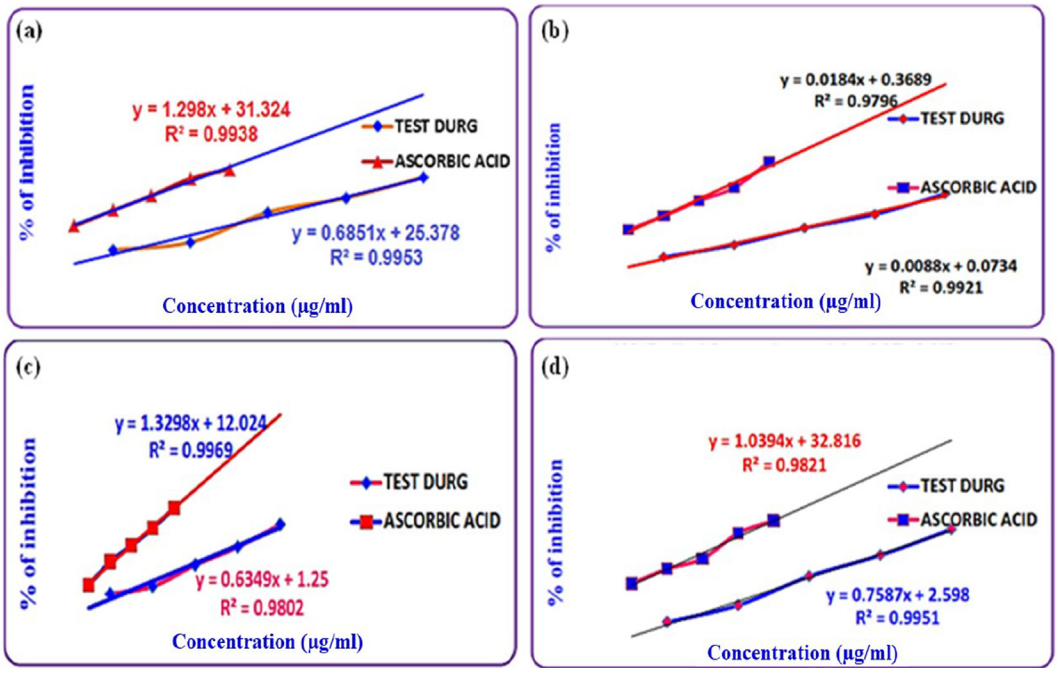

Fig. 6. Radical Scavenging activity of *Ae*-ZnONPs. a) DPPH assay; b) Reducing power assay; c) Hydrogen peroxide assay; d) Nitric Oxide assay.

Table 7
Reducing Power Assay of Activity of *Ae*-ZnONPs.

Treatment	Concentration (µg/mL)	OD AT 700 nm	IC_{50} value (µg/ml)
Ae-ZnONPs	100	0.9810	
	80	0.7501	56
	60	0.5964	
	40	0.4059	
	20	0.2732	
Ascorbic acid	50	1.3417	26
	40	1.0490	
	30	0.9022	
	20	0.7316	
	10	0.5803	

Table 8
H_2O_2 Radical scavenging activity of *Ae*-ZnONPs.

Treatment	Concentration (µg/ml)	% of inhibition	IC_{50} value (µg/ml)
Ae-ZnONPs	100	66.94 ± 1.6	76
	80	51.04 ± 0.5	
	60	38.26 ± 0.2	
	40	23.02 ± 0.7	
	20	17.46 ± 0.2	
Vitamin – C	50	78.62 ± 0.4	28
	40	64.36 ± 1.5	
	30	52.09 ± 0.7	
	20	40.42 ± 1.2	
	10	24.10 ± 0.3	

ciprofloxacin and showed 4 mm more inhibition zone against *Bacillus subtilis* when compared with standard.

Additionally, the particles possess good anti-inflammatory and antioxidant tendencies of nanoparticle cell interaction behaviour. The inhibition zone concentrations and IC_{50} are lower than the LC_{50} except for the reducing power assay IC_{50}. Global hardness is higher for the ZnO molecules and it won't be an excellent biological inhibitor. However, the prepared *Ae*-ZnONPs showed promising activity in all studies. These results confirmed that the particle size is a tiny and permeable character inside the pathogen's cell wall.

Table 9
NO assay of *Ae*-ZnONPs.

Treatment	Concentration (µg\ ml)	% of inhibition	IC_{50} value (µg/ml)
Ae-ZnONPs	100	79.20 ± 1.0	62
	80	62.59 ± 0.8	
	60	49.00 ± 1.5	
	40	30.37 ± 0.6	
	20	19.44 ± 0.1	
Vitamin- C	50	84.73 ± 14	16
	40	76.80 ± 1.0	
	30	61.43 ± 0.7	
	20	53.74 ± 1.3	
	10	44.29 ± 0.5	

This work successfully synthesized bioactive nanomaterial from the plant for future drug innovations, and materials that can be a drug were concluded.

Declaration of Competing Interest

The authors declare that they have no known competing financial interests or personal relationships that could have appeared to influence the work reported in this paper.

Acknowledgments

This work was funded by Researchers Supporting Project number (RSP-2021/27), King Saud University, Riyadh, Saudi Arabia.

References

Agi, A., Junin, R., Jaafar, M.Z., Mohsin, R., Arsad, A., Gbadamosi, A., Fung, C.K., Gbonhinbor, J., 2020. Synthesis and application of rice husk silica nanoparticles for chemical enhanced oil recovery. J. Mater. Res. Technol. 9 (6), 13054–13066. https://doi.org/10.1016/j.jmrt.2020.08.112.

Ahmad, S., Munir, S., Zeb, N., Ullah, A., Khan, B., Ali, J., Ali, S., 2019. Green nanotechnology: a review on green synthesis of silver nanoparticles - an ecofriendly approach. Int. J. Nanomed. 14, 5087–5107. https://doi.org/10.2147/IJN.S200254.

Alastruey, A.I., Melhem, M.S.C., Bonfietti, L.X., Rodriguez, J.L., 2015. Susceptibility test for fungi: clinical and laboratorial correlations in medical mycology. Rev. Inst. Med. Trop. Sao Paulo 57 (19), 57–64. https://doi.org/10.1590/S0036-46652015000700011.

Alenghat, F.J., 2013. Functional organization of vertebrate plasma membrane | membrane protein dynamics and functional implications in mammalian cells. Curr. Top. Membr. 72, 89–120. https://doi.org/10.1016/b978-0-12-417027-8.00003-9.

Anosike, C.A., Obidoa, O., Ezeanyika, L.U., 2012. Membrane stabilization as a mechanism of the anti-inflammatory activity of methanol extract of garden egg (*Solanumaethiopicum*). DARU J. Pharma. Sci. 20 (76), 1–7. https://doi.org/10.1186/2008-2231-20-76.

Arumugam, R., Vijayakumar, N., Mani, R., 2016. Effect of naringin on ammonium chloride-induced hyperammonemic rats: A dose-dependent study. J. Acute Med. 6 (3), 55–60. https://doi.org/10.1016/j.jacme.2016.08.001.

Baharara, J., Namvar, F., Ramezani, T., Hosseini, N., Mohamad, R., 2014. Green synthesis of silver nanoparticles using *Achilleabiebersteinii* flower extract and its anti-angiogenic properties in the rat aortic ring model. Molecules 19 (4), 4624–4634. https://doi.org/10.3390/molecules19044624.

Balalakshmi, C., Gopinath, K., Govindarajan, M., Lokesh, R., Arumugam, A., Alharbi, N.S., Kadaikunnan, S., Khaled, J.M., Benelli, G., 2017. Green synthesis of gold nanoparticles using a cheap *Sphaeranthus indicus* extract: impact on plant cells and the aquatic crustacean *Artemia* nauplii. J. Photochem. Photobiol. B: Biol. 173, 598–605. https://doi.org/10.1016/j.jphotobiol.2017.06.040.

Bodke, M.R., Purushotham, Y., Dole, B.N., 2018. Comparative study on zinc oxide nanocrystals synthesized by two precipitation methods. Cerâmica 64 (369), 91–96. https://doi.org/10.1590/0366-69132018643692207.

Bruska, M.K., Czekaj, I., Delley, B., Mantzaras, J., Wokaun, A., 2011. Electronic structure and oxygen vacancies in PdO and ZnO: validation of DFT models. PCCP 13 (35), 15947–15954. https://doi.org/10.1039/C1CP20923J.

Chen, Q., Espey, M.G., Sun, A.Y., Lee, J.H., Krishna, M.C., Shacter, E., Choyke, P.L., Pooput, C., Kirk, K.L., Buettner, G.R., Levine, M., 2007. Ascorbate in pharmacologic concentrations selectively generates ascorbate radical and hydrogen peroxide in extracellular fluid in vivo. Proc. Natl. Acad. Sci. 104 (21), 8749–8754. https://doi.org/10.1073/pnas.0702854104.

Cheng, T.H., Yang, Z.Y., Tang, R.C., Zhai, A.D., 2020. Functionalization of silk by silver nanoparticles synthesized using the aqueous extract from tea stem waste. J. Mater. Res. Technol. 9 (3), 4538–4549. https://doi.org/10.1016/j.jmrt.2020.02.081.

Chowdhury, A., Azam, S., Jainul, M.A., Faruq, K.O., Islam, A., 2014. Antibacterial activities and *in vitro* anti-Inflammatory (Membrane Stability) properties of methanolic extracts of *Gardenia coronaria* Leaves. Inter. J. Microbiol. 6, 1–5. https://doi.org/10.1155/2014/410935.

Christopher, S., Mathew, M., Liu, L., Urias, E., Yarema, K., 2015. Cell surface and membrane engineering: emerging technologies and applications. J. Funct. Biomater. 6, 454–485. https://doi.org/10.3390/jfb6020454.

Doan, T., Uyen, T., Nguyen, T.T., Thi, Y.D., Ta, T., Kieu, H., Phan, B.T., Kim, N., 2020. Green synthesis of ZnO nanoparticles using orange fruit peel extract for antibacterial activities. RSC Adv. 10, 23899–23907. https://doi.org/10.1039/d0ra04926c.

Faraz, M., Ansari, M., Khare, N., 2018. Synthesis of nanostructure manganese doped zinc oxide/polystyrene thin films with excellent stability, transparency and super-hydrophobicity. Mater. Chem. Phys. 211, 137–143. https://doi.org/10.1016/j.matchemphys.2018.02.011.

Fugh, B.A., 2000. Herb-drug interactions. Lancet 355 (9198), 134–138. https://doi.org/10.1016/S0140-6736(99)06457-0.

Gangwar, M., Gautam, M.K., Sharma, A.K., Tripathi, Y.B., Goel, R.K., Nath, G., 2014. Antioxidant capacity and radical scavenging effect of polyphenol rich *mallotus philippenensis* fruit extract on human erythrocytes: An In Vitro Study. Sci. World J. 2014, 1–12. https://doi.org/10.1155/2014/279451.

Govindarajan, M., Benelli, G., 2016. *Artemisia absinthium*-borne compounds as novel larvicides: effectiveness against six mosquito vectors and acute toxicity on non-target aquatic organisms. Parasitol. Res. 115 (12), 4649–4661. https://doi.org/10.1007/s00436-016-5257-1.

Govindarajan, M., Benelli, G., 2017. A facile one-pot synthesis of eco-friendly nanoparticles using *Carissa carandas*: Ovicidal and larvicidal potential on malaria, dengue and filariasis mosquito vectors. J. Cluster Sci. 28 (1), 15–36. https://doi.org/10.1007/s10876-016-1035-6.

Govindarajan, M., 2011. Evaluation of indigenous plant extracts against the malarial vector, *Anopheles stephensi* (Liston) (Diptera: Culicidae). Parasitol. Res. 109 (1), 93–103. https://doi.org/10.1007/s00436-010-2224-0.

Govindarajan, M., Khater, H.F., Panneerselvam, C., Benelli, G., 2016a. One-pot fabrication of silver nanocrystals using *Nicandra physalodes*: A novel route for mosquito vector control with moderate toxicity on non-target water bugs. Res. Vet. Sci. 107, 95–101. https://doi.org/10.1016/j.rvsc.2016.05.017.

Govindarajan, M., Rajeswary, M., Muthukumaran, U., Hoti, S.L., Khater, H.F., Benelli, G., 2016b. Single-step biosynthesis and characterization of silver nanoparticles using *Zornia diphylla* leaves: A potent eco-friendly tool against malaria and arbovirus vectors. J. Photochem. Photobiol. B: Biol. 161, 482–489. https://doi.org/10.1016/j.jphotobiol.2016.06.016.

Govindarajan, M., Sivakumar, R., Rajeswary, M., Veerakumar, K., 2013. Mosquito larvicidal activity of thymol from essential oil of *Coleus aromaticus* Benth. against *Culex tritaeniorhynchus, Aedes albopictus*, and *Anopheles subpictus* (Diptera: Culicidae). Parasitol. Res. 112 (11), 3713–3721. https://doi.org/10.1007/s00436-013-3557-2.

Gülçin, I., Huyut, Z., Elmastaş, M., Aboul-Enein, H.Y., 2010. Radical scavenging and antioxidant activity of tannic acid. Arab. J. Chem. 3 (1), 43–53. https://doi.org/10.1016/j.arabjc.2009.12.008.

Gunalan, S., Sivaraj, R., Rajendran, V., 2012. Green synthesized ZnO nanoparticles against bacterial and fungal pathogens. Prog. Nat. Sci. Mater. Int. 22 (6), 693–700. https://doi.org/10.1016/j.pnsc.2012.11.015.

Husen, A., Siddiqi, K., 2014. Phytosynthesis of nanoparticles: concept, controversy and application. Nanoscale Res. Lett. 9 (1), 229. https://doi.org/10.1186/1556-276x-9-229.

Indramahalakshmi, G., 2017. Characterization and antibacterial activity of zinc oxide nanoparticles synthesized using *Opuntia ficusindica* fruit aqueous extract. Asian J. Phys. Chem. Sci. 3 (2), 1–7. https://doi.org/10.9734/AJOPACS/2017/35917.

Iravani, S., 2011. Green synthesis of metal nanoparticles using plants. Green Chem. 13, 2638–2650. https://doi.org/10.1039/C1GC15386B.

Irshad, M., Zafaryab, M., Singh, M., Rizvi, M.M.A., 2012. Comparative analysis of the antioxidant activity of *cassia fistula* extracts. Int. J. Med. Chem. 2012, 1–6. https://doi.org/10.1155/2012/157125.

Jagtap, U.B., Bapat, V.A., 2013. Green synthesis of silver nanoparticles using *artocarpus heterophyllus* Lam. seed extract and its antibacterial activity. Ind. Crops Prod. 46, 132–137. https://doi.org/10.1016/j.indcrop.2013.01.019.

Janaki, A.C., Sailatha, E., Gunasekaran, A., 2015. Synthesis, characteristics and antimicrobial activity of ZnO nanoparticles. Spectrochim. Acta Part A: Mol. Biomol. Spectrosc. 144, 17–22. https://doi.org/10.1016/j.saa.2015.02.041.

Jayaprakash, R., Saroj Kumar, S., Hemalatha, S., Easwaramoorthy, D., 2016. QSAR, Brine shrimp lethal assay and antimicrobial studies on synthesized L-Tryptophan-2,4-dihydroxy benzaldehyde Schiff Base. Inter. J. Chem. Tech. Research. 9 (6), 48–54. https://doi.org/10.22159/ajpcr.2016.v9s3.14664.

Jin-Ming, K., Ngoh, K., Lian, S.C., Tet, F.C., 2003. Recent advances in traditional plant drugs and orchids. Acta Pharmacol. Sin. 24 (1), 7–21.

Kumari, S., Deori, M., Elancheran, R., Kotoky, J., Devi, R., 2016. *In vitro* and *in vivo* antioxidant, anti-hyper lipidemic properties and chemical characterization of *centellaasiatica* (L.) extract. Front. Pharmacol. 7, 1–12. https://doi.org/10.3389/fphar.2016.00400.

Li, W., Ji, S., Li, Y., Huang, A., Luo, H., Jin, P., 2014. Synthesis of VO_2 nanoparticles by a hydrothermal-assisted homogeneous precipitation approach for thermochromic applications. RSC Adv. 4 (25), 13026–13033. https://doi.org/10.1039/C3RA47666A.

Mariappan, P., Krishnamoorthy, K., Kadarkaraithangam, J., Govindasamy, M., 2011. Selective toxicity of ZnO nanoparticles toward Gram-positive bacteria and cancer cells by apoptosis through lipid peroxidation. Nanomedicine 7 (2), 184–192. https://doi.org/10.1016/j.nano.2010.10.001.

Mathivanan, T., Govindarajan, M., Elumalai, K., Krishnappa, K., Ananthan, A., 2010. Mosquito larvicidal and phytochemical properties of *Ervatamia coronaria* Stapf. (Family: Apocynaceae). J. Vector Borne Dis. 47 (3), 178–180.

Narayanan, K.B., Sakthivel, N., 2011. Green synthesis of biogenic metal nanoparticles by terrestrial and aquatic phototrophic and heterotrophic eukaryotes and biocompatible agents. Adv. in Colloid and Interface Sci. 169 (2), 59–79. https://doi.org/10.1016/j.cis.2011.08.004.

Naseer, A., Ali, A., Ali, S., Mahmood, A., Kusuma, H.S., Nazir, A., Yaseen, M., Khan, M.I., Ghaffar, A., Abbas, M., Iqbal, M., 2020. Biogenic and eco-benign synthesis of platinum nanoparticles (Pt NPs) using plants aqueous extracts and biological derivatives: environmental, biological and catalytic applications. J. Mater. Res. Technol. 9 (4), 9093–9107. https://doi.org/10.1016/j.jmrt.2020.06.013.

Nath, D., Banerjee, P., 2013. Green nanotechnology – A new hope for medical biology. Environ. Toxicol. Appl. Pharmacol. 36 (3), 997–1014. https://doi.org/10.1016/j.etap.2013.09.002.

Pant, K., Agarwal, K., Saini, P., 2012. To study *in vitro* anti-inflammatory activity of *anthracephalus cadamba* leaves extract. DHR Int. J. Pharma. Sci. 3, 55–60.

Ponvinobala, K., Kanchana, G., Rubalakshmi, G., 2012. *In vitro* antioxidant activity of hydro alcoholic extract of *andro graphisneesiana* leaves. J. Pharm. Res. 5, 1256–1259.

Priyanka, D., Prasanna, K., 2020. Concept and application of phytoremediation in the fight of heavy metal toxicity. J. Pharm. Sci. Res. 12 (6), 795–804.

Rahman, M.M., Islam, M.B., Biswas, M., 2015. *In vitro* antioxidant and free radical scavenging activity of different parts of *Tabebuia pallida* growing in Bangladesh. BMC Res. Notes 621 (8), 1–9. https://doi.org/10.1186/s13104-015-1618-6.

Raja, A., Ashokkumar, S., Pavithra Marthandam, R., Jayachandiran, J., Khatiwada, C. P., Kaviyarasu, K., Ganapathi Raman, R., Swaminathan, M., 2018. Eco-friendly preparation of zinc oxide nanoparticles using *Tabernaemontana divaricata* and its photocatalytic and antimicrobial activity. J. Photo. Chem. Photobiol B. 181, 53–58. https://doi.org/10.1016/j.jphotobiol.2018.02.011.

Rosi, N.L., Mirkin, C.A., 2005. Nanostructures in biodiagnostics. Chem. Rev. 105 (4), 1547–1562. https://doi.org/10.1021/cr030067f.

Roy, N., Gaur, A., Jain, A., Bhattacharya, S., Rani, V., 2013. Green synthesis of silver nanoparticles: An approach to overcome toxicity. Environ. Toxicol. Appl. Pharmacol. 36 (3), 807–812. https://doi.org/10.1016/j.etap.2013.07.005.

Selim, Y., Azb, M.A., Ragab, I., Abd El-Azim, H.M., 2020. Green synthesis of zinc oxide nanoparticles using aqueous extract of *Deverra tortuosa* and their cytotoxic activities. Sci. Rep. 10, 1–9. https://doi.org/10.1038/s41598-020-60541-1.

Sirelkhatim, A., Mahmud, S., Seeni, A., Kaus, N.H.M., Ann, L.C., Bakhori, S.K.M., Hasan, H., Mohamad, D., 2015. Review on zinc oxide nanoparticles: antibacterial activity and toxicity mechanism. Nano-Micro Lett. 7 (3), 219–242. https://doi.org/10.1007/s40820-015-0040-x.

Sonane, M., Moin, N., Satish, A., 2017. The role of antioxidants in attenuation of Caenorhabditis elegans lethality on exposure to TiO2 and ZnO nanoparticles. Chemosphere 187 (2017), 240–247. https://doi.org/10.1016/j.chemosphere.2017.08.080.

Suganya, P., Vaseeharan, B., Vijayakumar, S., Balan, B., Govindarajan, M., Alharbi, N.S., Kadaikunnan, S., Khaled, J.M., Benelli, G., 2017. Biopolymer zein-coated gold nanoparticles: synthesis, antibacterial potential, toxicity and histopathological effects against the Zika virus vector *Aedes aegypti*. J. Photochem. Photobiol. B: Biol. 173, 404–411. https://doi.org/10.1016/j.jphotobiol.2017.06.004.

Talam, S., Karumuri, R.S., Gunnam, N., 2012. Synthesis, characterization and spectroscopic properties of ZnO nanoparticles. ISRN Nanomater. 2021, 1–6. https://doi.org/10.5402/2012/372505.

Wei, J., Hamid, M., Baoshan, X., 2009. Bacterial toxicity comparison between nano- and micro-scaled oxide particles. Environ. Pollut. 157 (5), 1619–1625. https://doi.org/10.1016/j.envpol.2008.12.025.

Yuan, H., Ma, Q., Ye, L., Piao, G., 2016. The traditional medicine and modern medicine from natural products. Molecules 21 (5), 1–18. https://doi.org/10.3390/molecules21050559.

Further Reading

Ajithadas, A., Ramraj, N., Venkatachalam, K., Pandi, B., 2015. Synthesis and characterization of silver nanoparticles of insulin plant (*costus pictus* d. don) Leaves. Asian J. Biomed. Pharmaceut. Sci. 4 (34), 1–6. https://doi.org/10.15272/ajbps.v4i34.532.

Balasooriya, E.R., Jayasinghe, C.D., Jayawardena, U.A., Ruwanthika, R.W.D., Mendis, S.R., Udagama, P.V., 2017. Honey mediated green synthesis of nanoparticles: New era of safe nanotechnology. J. Nanomater. 23, 1–10. https://doi.org/10.1155/2017/5919836.

Kalpana, V.N., Devi Rajeswari, V., 2018. Review on green synthesis, biomedical applications, and toxicity studies of ZnO NPs. Bioinorg. Chem. Appl. 2018, 1–12. https://doi.org/10.1155/2018/3569758.

Senthilkumar, N., Nandhakumar, E., Priya, P., Soni, D., Vimalan, M., Vetha Potheher, I., 2017. Synthesis of Zno nanoparticles using leaf extract of *Tectona grandis* (L.) and their antibacterial, anti-arthritic, antioxidant and in vitro cytotoxicity activities. New J. Chem. 41 (18), 10347–10356. https://doi.org/10.1039/C7NJ02664A.